

Quantum chaos in disordered graphene

I. Amanatidis and S.N. Evangelou*

Department of Physics, University of Ioannina, Ioannina 45110, Greece

We have studied numerically the statistics for electronic states (level-spacings and participation ratios) from disordered graphene of finite size, described by the aspect ratio W/L and various geometries, including finite or toroidal, chiral or achiral carbon nanotubes. Quantum chaotic Wigner energy level-spacing distribution is found for weak disorder, even infinitesimally small disorder for wide and short samples ($W/L \gg 1$), while for strong disorder Anderson localization with Poisson level-statistics always sets in. Although pure graphene near the Dirac point corresponds to integrable ballistic statistics chaotic diffusive behavior is more common for realistic samples.

PACS numbers: 73.22.Dj,73.63.-b,73.20.Fz,81.05.Uw

I. INTRODUCTION

During the last few years theoretical and experimental interest has grown immensely on monolayer graphite samples, known as graphene following its pioneering fabrication [1, 2, 3]. This remarkable two-dimensional (2D) honeycomb lattice structure made of carbon atoms behaves rather differently from ordinary 2D metals. Its most interesting quantum property is a linear dispersion near the Fermi energy, known as the Dirac point, where the conduction and valence bands of graphene touch each other, with the low-lying excitations behaving as massless Dirac fermions. Anomalous integer quantum Hall effect for graphene has been observed [2, 4], which depends on the symmetry of introduced disorder [5] and has been discussed in terms of relativistic Dirac theory[6]. Due to its extraordinary properties, such as high mobility, current-carrying capacity and thermal conduction, graphene is regarded as a good candidate to replace silicon in future nanoelectronics [7]. The possibility of gating and processing graphene sheets into multi-terminal devices is also an intriguing issue for related research [8].

The purpose of this paper is to examine the energy level-statistics for finite graphene sheets (quantum dots in the form of nanotubes) [9], for width W and length L characterized by their aspect ratio W/L . We have also considered various directions of graphene and various sorts of boundary conditions (BC), in the presence of disorder. Although graphene is widely regarded as a rather clean material it is believed that mild disorder should exist [10, 11, 12, 13, 14, 15]. For example, alloy type disorder from placing at random different lattice atoms or vacancies in the honeycomb lattice [13], or correlated disorder [14]. The latter, by changing the universality class from orthogonal to symplectic [14], is expected to lead to unusual phenomena, such as weak anti-localization with

metallic behavior at the Dirac point. The usual short-ranged disorder causes localization also in graphene [15], which can limit the performance of graphene made devices. These effects of disorder naturally reflect on the conduction of electrons, which can be studied by usual scattering methods for electron waves in graphene billiards [16]. Near the Dirac point, where the density of states for pure graphene vanishes, the transmission becomes pseudo-diffusive in the limit ($W/L \gg 1$) independently of BC [17].

Recent experimental observations for size quantization of electron levels in graphene quantum dots [18] led to theoretical consideration of level-statistics in tight-binding models[19]. These numerical simulations for special geometries of the honeycomb lattice (named Dirac billiards, with geometrical shapes such as weakly disordered circle or triangle) are in reasonable agreement with the observed level-statistics in the experiment [18]. It was found that weak disorder at the edges of the sample can also produce quantum chaos, which is independent of the shape of graphene dots. Our results agree with these observations [18, 19] since we have also obtained Poisson (integrable) level-statistics in the clean limit, which becomes chaotic for weak disorder, independently of geometry. Moreover, our study which was carried out for all strengths of disorder finds quantum chaotic behavior for wide and short nanotubes ($W/L \gg 1$) even in the infinitesimally small disorder limit, confirming the presence of pseudo-diffusive behavior in this case. In the opposite limit of narrow long cylinders ($W/L \ll 1$) the statistics becomes ballistic δ -function type, similar to that of the one-dimensional (1D) chain. In other words, for realistic samples having arbitrary small disorder the outstanding ballistic behavior of long nanotubes is replaced by diffusive chaotic behavior for short and wide graphene samples.

The paper is organized as follows: In Sec. II we introduce the graphene lattices studied. They are of various sizes and geometries, corresponding to chiral and achiral carbon nanotubes. Their tight-binding Hamiltonian

*e-mail:sevagel@cc.uoi.gr

in the presence of disorder is introduced. In Sec. III we show that for diagonal and off-diagonal disorder (in the case of large W/L even for infinitesimally small disorder) Wigner chaotic level-statistics is obtained while for strong disorder it becomes Poisson, independently of the type of graphene sheet. Our results for the participation ratio complement these findings by showing extended eigenstates close to the Dirac point and confirm the presence of Anderson localization for strong disorder. Finally, in Sec. IV we summarize our main conclusions.

II. THE TIGHT BINDING HAMILTONIAN

The tight-binding Hamiltonian of π bonding in graphene is

$$H = \sum_i \varepsilon_i c_i^\dagger c_i - \gamma \sum_{\langle i,j \rangle} (c_i^\dagger c_j + c_j^\dagger c_i), \quad (1)$$

where $c_i (c_i^\dagger)$ annihilates (creates) an electron at the sites of the honeycomb lattice, ε_i represents the on site energy which in the case of diagonal disorder is a random number in the range $[-w/2, w/2]$, where w denotes the disorder. For off-diagonal disorder $\varepsilon_i = 0$ and the logarithm of the nearest neighbor hopping element γ takes random values in the range $[-w/2, w/2]$ [20].

In the case of periodic BC only in one direction, the other being much longer with hard wall BC, the graphene samples represent finite single wall carbon nanotubes with $W/L \ll 1$ [9]. These are effectively one-dimensional objects, build up by wrapping sheets of graphene into very long cylinders, and in modern technology underpin the evolution to nano-electronics. Their electronic properties depend on the wrapping direction which is characterized by the so-called chiral vector (n,m) , expressed in terms of graphene primitive unit lattice vectors \vec{a}_1, \vec{a}_2 , $|\vec{a}_1| = |\vec{a}_2| = \sqrt{3}a_{C-C} = a$, where a_{C-C} is the distance between two atoms and a the honeycomb lattice constant. Since various possibilities exist to roll up graphene, depending on the rolling direction one obtains armchair, zig-zag and chiral nanotubes [9]. The armchair nanotubes characterized by a chiral vector (n,n) can be obtained by rolling the graphene sheet along one of the three vectors joining a honeycomb lattice site to its nearest-neighbors. The perimeter of the (n,n) armchair nanotubes consists of n hexagons along the rolling direction connected by n single bonds and they are always metallic. The $(n,0)$ zig-zag nanotubes are defined by a rotation of the graphene sheet by 90° and the n hexagons followed by n single bonds lie now along the longitudinal axis of the tube (the rolling direction is perpendicular). The $(n,0)$ nanotubes are metallic only when n is a multiple of 3. In all other cases, that is rotating the graphene sheet in between the previous two and then rolling it up,

is equivalent to placing the hexagons followed by single bonds along intermediate directions. This third type of carbon nanotubes is called chiral (n,m) , $n \neq m$ and its band structure is metallic only when $n - m$ is a multiple of 3 [9].

Our approach consists of studying the effects of disorder in graphene by obtaining numerically the eigenvalues and eigenvectors of the Hamiltonian H in the presence of disorder. In our computations we have fixed the short-ranged site (diagonal) and bond (off-diagonal) type disorder for many random samples. The statistics of the obtained eigen-solutions are subsequently analyzed in order to address the quantum chaos issues. Since for the (n,n) armchair nanotube a unit cell along its long direction consists of two slices around the tube, (with $2n$ carbon atoms each making $4n$ atoms in total the total number of hexagons covering the unit cell is $N_{hex} = 2n$). The number of such unit cells along a finite nanotube is N_c so that their size can be classified in terms of n and N_c .

In the absence of disorder ($w = 0$) the dispersion of pure graphene sheet taken in the correct orientation, that of armchair nanotubes along the x -axis with their rolling direction along the vertical y -axis, is [21]

$$E(k_x, k_y) = \pm \gamma \left(1 + 4 \cos\left(\frac{\sqrt{3}k_y a}{2}\right) \cos\left(\frac{k_x a}{2}\right) + 4 \cos^2\left(\frac{k_x a}{2}\right) \right)^{1/2}, \quad (2)$$

with quantized values of $\mathbf{k} = (k_x, k_y)$. For a finite armchair nanotube (periodic BC along y and hard wall BC along x) the eigenstates are labelled by two integers, via

$$k_x a = \frac{\pi}{N_c + \frac{1}{2}} j_x, \quad k_y a = \frac{2\pi}{\sqrt{3}n} j_y, \quad (3)$$

with $j_x = 1, \dots, N_c$ and $j_y = 1, \dots, 2n$. The output is $2nN_c$ positive and exactly equal negative eigenvalues (a fact of sublattice symmetry [22], since the two types of atoms A and B in graphene for nearest neighbor hopping make two interconnected A and B sublattices). In the case of infinite nanotubes the $k_x a$ quantization of Eq. (3) does not arise and the band structure of Eq. (2) becomes one-dimensional, a function of k_x only [9]. For toroidal armchair nanotubes, where appropriate periodic BC are imposed also along the longitudinal direction $k_x a = \frac{2\pi}{N_c} j_x$, $j_x = 1, \dots, N_c$.

For the more general chiral (n,m) , $n \neq m$ nanotubes the quantized component of the wave vector (n,m) along the perimeter of the nanotube where periodic BC are imposed, satisfies

$$k_y a = \frac{2\pi}{W/a} j_y, \quad j_y = 1, \dots, N_{hex}, \quad (4)$$

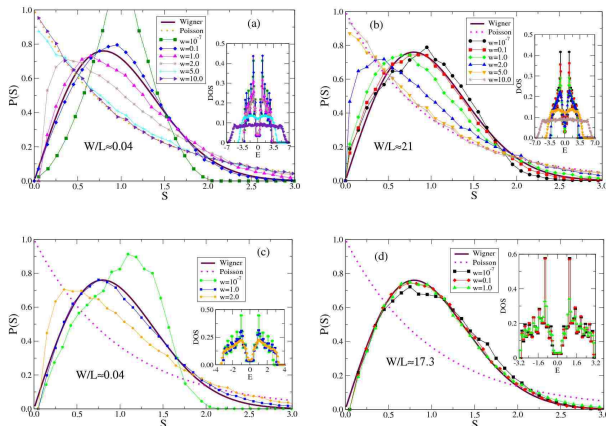


FIG. 1: The normalized level-spacing distribution function $P(S)$ from 10 samples of graphene with diagonal disorder (for the values of disorder strength w see figure): **(a)** For graphene structures with a very small aspect ratio $W/L \approx 0.04$ and 4960 sites corresponding to $N_c = 40$ unit cells of the chiral (7,4) nanotube. As the disorder strength increases a gradual crossover is seen, from a broad δ -function (in the form of a Gaussian around the mean) for clean nanotubes to a Poisson distribution for strong disorder. **(b)** The same as in (a) but for a wide and short chiral (36,180) nanotube with $N_c = 1$ having aspect ratio $W/L \approx 21$ (4464 sites). In this case the distribution is close to Wigner even for almost zero disorder. **(c),(d)** From the (7,4) and (36,120) toroidal nanotube geometries consisting of $N_c = 40, 12$ unit cells corresponding to aspect ratios $W/L \approx 0.04, 17.3$ and sites 4960, 5760 sites, respectively. In the insets the densities of states are shown with the characteristic dip near the Dirac point, which remains for weak disorder but closes for strong disorder ($w > 3$), leading to a broad density of localized states.

having width $W = a\sqrt{n^2 + m^2 + nm}$ given by their perimeter and $N_{hex} = 2L^2/(a^2d_r)$ hexagons in a unit cell of length $|\mathbf{T}| = \sqrt{3}W/d_r$, d_r being the greatest common divisor of $2m+n$ and $2n+m$. For a given value of the quantized k_y the energy of an infinite chiral nanotube is a function of the continuous longitudinal component k_x only, with $-\frac{\pi}{|\mathbf{T}|} < k_x < +\frac{\pi}{|\mathbf{T}|}$. For armchair nanotubes (n,n) the unit cell reduces to width $W = a\sqrt{3}n$, length $|\mathbf{T}| = a$ and $N_{hex} = 2n$. Since $L = N_c a$ for N_c unit cells the considered aspect ratio is $W/L = d_r/(\sqrt{3}N_c)$ for chiral (n,m) nanotubes, reducing to $W/L = \sqrt{3}n/N_c$ for armchair (n,n) nanotubes.

III. RESULTS

Pure graphene sheets

Numerical computations of the eigen-solutions are required for chiral nanotubes even in the absence of disorder, since their unit cell along the tube can become

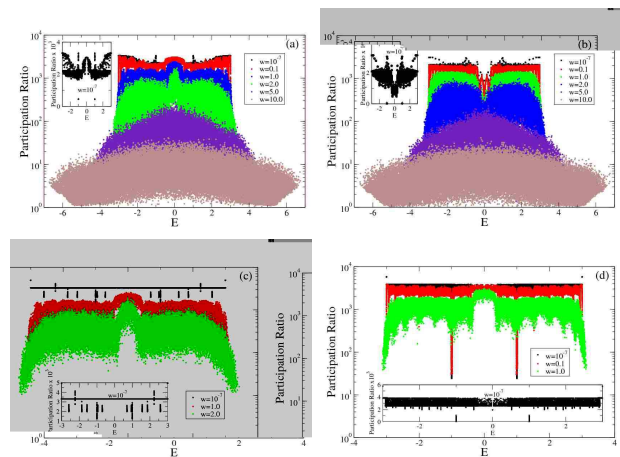


FIG. 2: For the same parameters as in Fig.1, but for the participation ratios of the corresponding eigenstates versus energy. The participation ratios indicate the number of sites where each eigenstate has a significant amplitude. For a perfect extended state its value should be ≈ 5000 sites for the chosen sizes. In the insets the results for pure graphene $w = 0$ are magnified, note the linear scale on the y -axis.

arbitrarily large depending on (n,m). For pure graphene we have found the expected ballistic behavior manifested via integrable Poisson statistics for arbitrary W/L , which becomes ballistic 1D-like in the limit $W/L \ll 1$. This can be simply understood near the Dirac point where the density of states is linear. In this regime the integrated density of states is $\mathcal{N}(E) \propto E^2$. Therefore, the statistics of the energy levels E should be replaced by the statistics of the unfolded squared levels E^2 which is required in order to make the density of states constant by fixing the mean level-spacing. If we use the usual quadratic dispersion for the squared levels $E^2 \propto k_x^2 + k_y^2$ the statistic near the Dirac point becomes equivalent to the statistics of integrable billiards [23], with E^2 replaced by E from

$$E_{j_x, j_y} = \alpha j_x^2 + j_y^2, \quad j_x, j_y \text{ integers}, \quad (5)$$

α being an irrational number fixed by the size of the adopted sample. The resulting statistics for zero disorder is obviously Poisson [23], except for very long samples in the 1D limit where the sum of Eq. (5) should depend on one parameter only and the corresponding level statistics becomes a trivial δ -function. We have verified this behavior, in agreement with [19]. However, for infinitesimally small disorder as seen in Fig. 1(b) the statistics changes and becomes chaotic when W/L is large (Wigner distribution) while it remains trivial ballistic 1D-like for small W/L shown in Fig. 1(a) (broad δ -function). In the almost clean limit, the ballistic behavior for small W/L is replaced by chaotic diffusive for larger W/L samples.

In the insets of Fig. 2 the behavior of the corresponding eigenstates for pure graphene can be seen on a linear scale, via their participation ratios. The main observa-

tion is that for the small W/L (Fig. 2(a) inset) the majority of ballistic states have a higher participation ratios when compared to those with large W/L (Fig. 2(b) inset). The distribution of the participation values becomes sharper for the small W/L torroidal nanotubes (Fig. 2(c) inset) when compared to large W/L (2(d) inset).

Diagonal and off-diagonal disorder

The density of states and the level-spacing distribution function $P(S)$ are computed for various graphene sheets with aspect ratios W/L , including chiral nanotubes. The corresponding nearest-level spacing distribution function is illustrated for different values of diagonal disorder in Fig. 1. All the unfolded energy levels in the band are considered for 10 runs, making the density of states constant everywhere in the band. No significant difference was found when levels near the Dirac point are considered only. For small W/L (Fig. 1(a)) the level spacing distribution function $P(S)$ is shown to vary from a broad δ -function like curve for almost zero disorder ($w = 10^{-7}$) towards the Poisson localized limit for strong disorder $w \gg$. For large W/L we observe instead (Figs. 1(b),(d)) a crossover not from a δ -function but from a Wigner chaotic distribution towards the localized Poisson limit in the strong disorder limit ($w \gg$). In the insets of Fig. 1 the corresponding average density of states is shown with the dip near the Dirac point, which disappears when the disorder increases.

In Fig. 2 we demonstrate the participation ratio which measures the extend of the corresponding eigenstates on the lattice. Near the Dirac point the values are seen to be higher for small W/L (Fig. 2(a)) when compared to large W/L (Fig. 2(b)). This observation is related to the observed δ -function and Wigner $P(S)$ distributions in Fig. 1, for small and large W/L , respectively. Similar results are obtained for torroidal nanotubes (Fig. 2(c) and (d)). For strong disorder our results indicate localization of all the states in the band with their participation ratio becoming small.

Off-diagonal disorder preserves chiral symmetry since it connects one sublattice to the other [20]. In Fig. 3 we show our results for the chiral (7,4) nanotube with off-diagonal disorder in the small $W \ll L$ nanotube limit. Fig 3(a) shows $P(S)$ (with the density of states in the inset) and fig. 3(b) the participation ratio of the corresponding eigenstates. Similar results are obtained to the diagonal disorder case, with the exception of the appearance of a singularity in the density of states, which develops at the band center (not seen in the figure due to scale) [20].

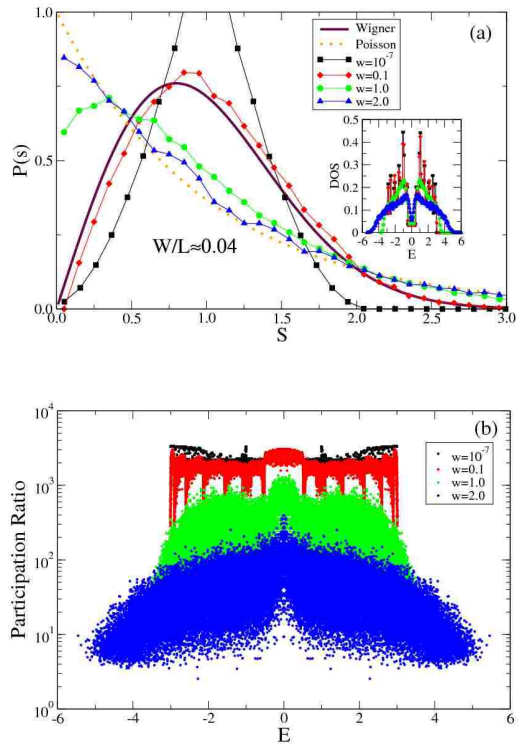


FIG. 3: **(a)** The level-spacing distribution function $P(S)$ and **(b)** the participation ratio for off-diagonal disorder of strength w (see figure) for the small aspect ratio $W/L \approx 0.04$ chiral (7,4) nanotube geometry of $N_c = 40$ cells (4960 sites).

IV. DISCUSSION

It is known that the band structure of graphene is metallic without a gap, having a density of states which becomes zero at the Dirac point. However, depending on the geometry of the samples a small gap can open near the Dirac point, e.g. for the (n,m) nanotubes which become insulating when $n - m$ is not a multiple of 3. Our study of the eigensolution statistics for various geometries specified by the aspect ratio W/L in the presence of disorder reveals some interesting features: First, quantum chaos becomes relevant also for weakly disordered graphene, with pseudo-diffusive Wigner statistics even for almost zero disorder when W/L is large. Second, for strong disorder localization occurs for all states in the band, in agreement with finite-size scaling transfer matrix studies at the Dirac point. Third, near the Dirac point, due to the linearity of density of states of pure graphene, a natural unfolding of levels corresponds to the study of squares of energies E^2 which gives integrable irrational billiard statistics. However, the pseudo-diffusive quantum chaotic behavior of graphene for infinitesimally small disorder independently of BC, for large aspect ratio W/L should become obvious in scattering experiments

from nanotubes.

Since infinitesimal disorder is inevitable also for graphene the question whether ballistic or diffusive behavior prevails can be answered in favor of a simple 1D-like ballistic behavior for small W/L and pseudo-diffusive for large W/L . For weak disorder quantum chaos and for strong disorder localization occurs, in agreement with other 2D disordered lattices. In conclusion, our computations for graphene in the presence of disorder show quantum chaos or Anderson localization for weak disorder (even almost zero disorder for large W/L) or strong disorder, respectively. This demonstration of quantum chaos in graphene is in agreement with recent theoretical and experimental studies.

-
- [1] K.S. Novoselov et al, Science **306**, 666 (2004).
 [2] K.S. Novoselov et al, Nature **438**, 197 (2005).
 [3] A.K. Geim and K.S. Novoselov, Nat. Mat. **6**, 183 (2007).
 [4] Y. Zhang, Y.W. Tan, H.L. Stormer and P. Kim, Nature **438**, 201 (2005).
 [5] P.M. Ostrovsky, I.V. Gornyi and A.D. Mirlin, Phys. Rev. B **77** 195430 (2008).
 [6] V.P. Gusynin and S.G. Shaparov, Phys. Rev. Lett. **95**, 146801 (2005).
 [7] C. Berger et al., Science **312**, 1191 (2006).
 [8] C. Berger et al., J. Phys. Chem. B **108**, 19912 (2004).
 [9] R. Saito, G. Dresselhaus, and M.S. Dresselhaus, *Physical Properties of Carbon Nanotubes* (Imperial College Press, London, 1998).
 [10] J.C.T. White and T.N. Todorov, Nature (London) **393**, 240 (1998).
 [11] M. Hjot and S. Stafstrm, Phys. Rev. B, **63**, 113406 (2001).
 [12] A. Atland, Phys. Rev. Lett. **97**, 236802 (2006).
 [13] N.M.R. Peres, F. Guinea, A.H. Castro Neto, Phys. Rev. B **73**, 125411 (2006).
 [14] P.M. Ostrovsky, I.V. Gornyi and A.D. Mirlin, Eur. Phys. J. Special Topics **148**, 63 (2007).
 [15] S.-J. Xiong and Y. Xiong, Phys. Rev. B **76**, 214204 (2007).
 [16] F. Miao et al Science **317**, 1530 (2007).
 [17] J. Tworzydlo et al, Phys. Rev. Lett., **96**, 246802 (2006).
 [18] L.A. Ponomarenko et al, Science **320** (2008).
 [19] H. De Raedt and M.I. Katselson, arXiv:0804.2758 [cond-mat.mes-hall]
 [20] S.N. Evangelou and D.E. Katsanos, J. Phys. A: Math. and Gen. **36**, 3237 (2003).
 [21] C. Bena and G. Montambaux, arXiv:0712.0765.
 [22] M. Inui, S.A. Trugman and E. Abrahams Phys. Rev. B **49** 3190 (1994).
 [23] G. Casati, B.V. Chirikov and I. Guarneri, Phys. Rev. Lett. **54**, 1350 (1983).